

## Silica banding in the deep-sea lithistid sponge *Corallistes undulatus*: Investigating the potential influence of diet and environment on growth

Michael J. Ellwood<sup>1</sup>

National Institute of Atmospheric and Water Research (NIWA) Ltd., P.O. Box 11-115, Hillcrest, Hamilton, New Zealand

Michelle Kelly

National Centre for Aquatic Biodiversity & Biosecurity, National Institute of Atmospheric and Water Research (NIWA) Ltd., Auckland, New Zealand

Bertrand Richer de Forges

UMR Systématique, adaptation, évolution, équipe Biogéographie marine tropicale, Institut de Recherche pour le Développement, Nouméa Cedex, Nouvelle-Calédonie

### Abstract

We present detailed records of trace metals and carbon isotopes to understand siliceous spicule formation in the deep-sea lithistid sponge *Corallistes undulatus* Lévi and Lévi, 1983 (Demospongiae: Corallistidae). X-ray analysis of two longitudinal sections removed from the lamellae of the cup-shaped sponge revealed 144 and 137 light and dark density band-pairs, respectively, within the siliceous skeleton. Four portions of silica were removed along one of the sections for silicon-32 (<sup>32</sup>Si) dating in order to constrain the overall extension rate of the sponge. Although there was some variability in the <sup>32</sup>Si data, the overall age established using these data indicated that the sponge was between 135 and 160 yr old. This agreed well with the counts of density band-pairs, indicating that these band-pairs represent an annual deposition of layers of silica in the desma skeleton. Links between silica deposition and growth (food supply) were established using the  $\Delta^{14}\text{C}$  and  $\delta^{13}\text{C}$  signatures of organic material trapped with the spicule matrix and the zinc content of the silica. A carbon budget based on these results indicated that the amount of fresh, labile surface export organic carbon reaching *C. undulatus* was not sufficient to support its growth. The  $\Delta^{14}\text{C}$  results for organic carbon trapped in the silica desmas, deposited after the 1960s, supports this assertion; only a small atmospheric nuclear weapons 'bomb' spike was observed in the  $\Delta^{14}\text{C}$  data. Taken together, the  $\Delta^{14}\text{C}$ ,  $\delta^{13}\text{C}$ , and trace-metal results all indicate that the organic carbon source to *C. undulatus* is likely to be a mixture of fresh, labile, surface-derived material and older, perhaps sediment-derived material, with the latter being dominant.

<sup>1</sup>To whom correspondence should be addressed. Present address: Department of Earth and Marine Sciences & Research School of Earth Sciences, The Australia National University, Canberra, ACT 0200, Australia (michael.ellwood@anu.edu.au).

### Acknowledgments

Research on the south New Caledonian slope was carried out onboard the New Caledonian IRD R/V *Alis*. M.K. thanks Captain Raymond Proner and his crew for their help during the voyage. M.K. particularly acknowledges the assistance of Cécile Debitus and Dominique Laurent from the Chemical Product Study Program (SMIB), Institut Français de Recherche Scientifique pour le Développement en Coopération, Noumea, New Caledonia, for arranging her participation in this voyage. We are grateful to Uwe Morgenstern, Institute of Geological and Nuclear Sciences, and Christine Prior, Rafter Radiocarbon Laboratory, Lower Hutt, New Zealand, for provision of <sup>32</sup>silicon dating and the <sup>14</sup>carbon dating services. CLIVAR and the Carbon Hydrographic Data Office (whpo.ucsd.edu) are acknowledged for allowing us to use the nutrient and temperature data from section P06W collected from the R/V *Knorr*, cruise number 138, leg 5. Finally, we thank Gitai Yahel and an anonymous reviewer for suggestions that helped to improve the manuscript.

This collaborative work was carried out with the financial assistance of the French Foreign Affairs Ministry through the IRD research teams. This research was supported with a New Zealand Foundation for Research Science & Technology Postdoctoral Fellowship to M.J.E.

The formation of siliceous spicules in marine sponges is not well understood. Recent work detailing the formation of siliceous spicules in the hexactinellid sponge *Euplectella* sp. appears to involve the nanometer-scale deposition of silica spheres around a central axial filament to form concentric rings separated by an organic matrix that provides flexibility, thereby reducing the chance of spicule fracture (Levi et al. 1989; Sundar et al. 2003; Aizenberg et al. 2005). Like hexactinellid sponges, lithistid sponges also contain siliceous skeletons comprising spicules. These spicules (desmas) interlock, rendering the skeleton rigid and often stony (Kelly 2000, 2003). At present little is known about the deposition of silica within this taxonomic order.

Lithistid sponges are commonly found on tropical and temperate seamounts and continental margins down to depths of about 1,000 m (Lévi and Lévi 1983; Kelly 2000; Pomponi et al. 2001). Several southwest Pacific species, including *Corallistes undulatus* Lévi and Lévi, *Neoschrammeniella fulvodesmus* (Lévi and Lévi), *Leidermatium pfeifferae* Wilson, and *Aciculites pulchra* Dendy, form large cups, bowls, and plates that extend linearly from the sponge margin (see Kelly in press). Close inspection of the lamellae show irregular or concentric ridges, indicating that silica deposition is not continuous but rather variable in nature (Fig. 1).

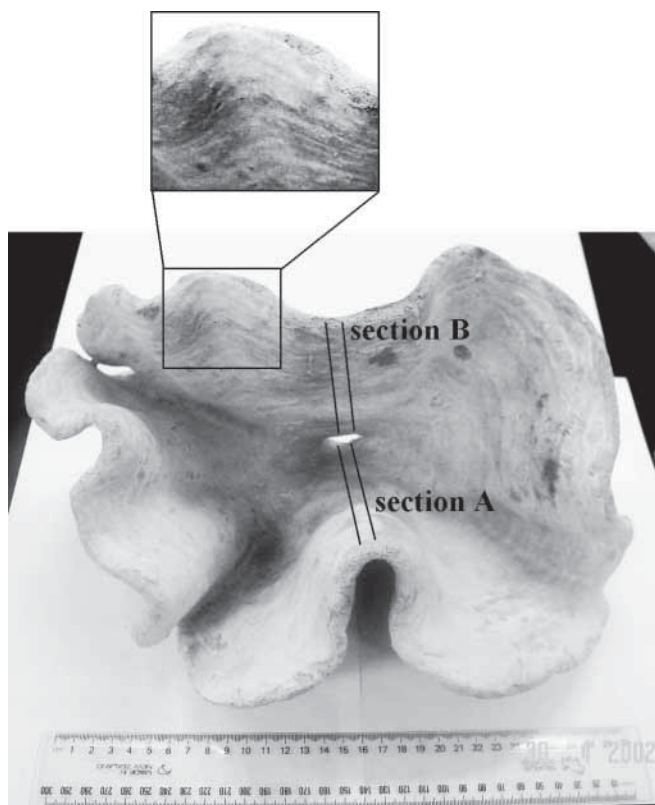


Fig. 1. *Corallistes undulatus* Lévi and Lévi, 1983 ('Lithistid' Demospongiae: Corallistidae). The inset highlights ridges of silica running parallel to the rim of the lamella. The segments for  $^{32}\text{Si}$  dating were adjacent to section A. Trace metals along with silicon were measured on approximately 1-mm-thick slices (15–50 mg) removed from section B.

The supply of organic carbon to benthic communities is an important determinant of population size, community distribution and structure, and the growth of constituent organisms. Supply of organic carbon might therefore influence the formation of silica growth bands in *C. undulatus* (Billet et al. 1983; Gooday and Turley 1990; Tyler 1995). In this study we investigated the nature and number of the silica ridges or bands using X-ray analysis of sections removed from the lamella of *C. undulatus*. The numbers of band-pairs observed were complemented by silicon-32 ( $^{32}\text{Si}$ ),  $\Delta^{14}\text{C}$  (C),  $\delta^{13}\text{C}$ , and trace-metal measurements to age the sponge and to better understand carbon sources to the sponge.

## Methods

**Sponge material**—A large, undulating, bowl-shaped lithistid sponge was obtained in 1999 from the northeastern side of 'Eponge Seamount' on the south New Caledonian slope of the Norfolk Ridge (24°54.24'S, 168°21.35'E) (Fig. 2). The sponge was collected from a depth of 540 m using a rock dredge deployed from the R/V *Alis* (Institut Français de Recherche Scientifique pour le Développement en Coopération, Noumea, New Caledonia) and was alive upon collection. The sponge forms a large foliose bowl ca.

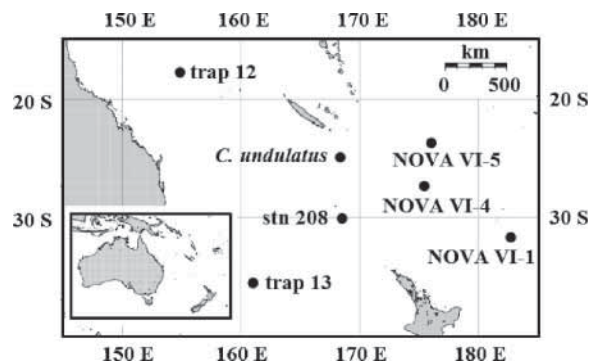


Fig. 2. Specimen collection locality, NOVA stations, nutrient station 208-P06W and sediment trap sites 12 and 13 (Kawahata and Ohta 2000).

30 cm wide and ca. 20 cm high, the sides of which are about 5–10 mm thick (Fig. 1). Like most lithistid sponges, this species is characterized by the presence of a heavily siliceous skeleton composed of desma spicules, the arms (clones) of which interlock (zygose) with adjacent desmas at their termini (Fig. 3) (see Kelly 2000).

**Enumeration of X-ray silica density bands**—Two 1-cm-thick sections were removed from the sponge lamella parallel to the axis of growth (toward the external margin), but these sections were removed from opposite sides of the bowl (Fig. 1). Sections were X-rayed using a conventional X-ray system with a 1-min exposure at 80 kV (ATC). The alternating light and dark density band-pairs seen in X-rayed sections (Fig. 4) were counted first with the unaided eye and secondly with the computer program Coral X-radiograph Densitometry System (CoralXDS, www.nova.edu/ocean/coralxds).

**$^{32}\text{Si}$  activity**— $^{32}\text{Si}$  is produced in the atmosphere by the spallation of argon following cosmic ray impact (Lal et al. 1960). This isotope is particularly useful for tracing siliceous sponge growth, as it has a half-life of  $140 \pm 10$  yr, which appears to be well within the life-history of many sponge species (Lal et al. 1970; Morgenstern et al. 2001). Briefly, four 1.4–2.1-cm segments (~5 g) were removed from the sponge lamella along the axis of growth adjacent to section A (Fig. 1) and were  $^{32}\text{Si}$ -dated under contract by the Institute for Geological and Nuclear Sciences in New Zealand. The segments were dissolved in a hot sodium hydroxide solution and separated from impurities by centrifuging and filtering, according to the methods of Morgenstern et al. (2001) and Lal et al. (1970). The dissolved silica was precipitated by the addition of hydrochloric acid. The dissolution and re-precipitation process was repeated an additional two times. Biogenic silica was recovered quantitatively. The purified silica was combusted overnight at 800°C, resulting in its transformation to a pure, fine, white powder. After a suitable in-growth period—about 3 months for  $^{32}\text{P}$  generation (the daughter product of  $^{32}\text{Si}$ )—the silica was dissolved in a strong NaOH solution, after which  $^{32}\text{P}$  was 'milked' from the solution by co-precipitation with a stable

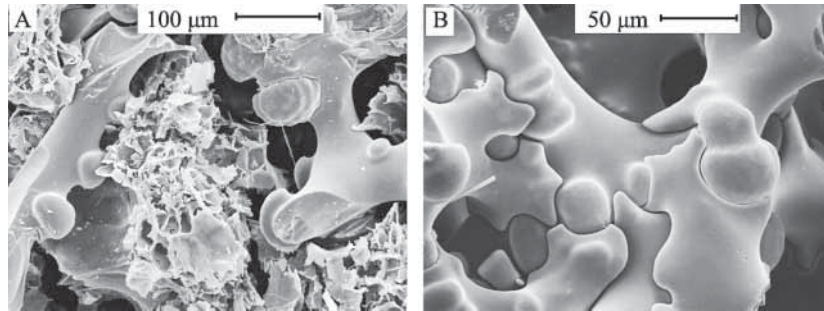


Fig. 3. SEM images of (A) intact uncleaned sample with dehydrated cellular mesohyl and (B) a cleaned sample, used for trace-metal analysis. Note the articulation (zygosis) of the adjacent desma spicules.

phosphorus carrier. Once milked,  $^{32}\text{P}$  activities were measured over several weeks in a low-background  $\beta$  counter (Quantulus; Perkin Elmer). The process of  $^{32}\text{Si}$  purification,  $^{32}\text{P}$  milking, and  $\beta$  counting takes approximately 4 months per sample. Errors associated with the  $\beta$  counter are based on counting statistics.

**Trace metals and silicon**—Iron, zinc (Zn), and aluminum, along with silicon, were measured on approximately 1-mm-thick slices (15–50 mg) removed from section B using methods previously published for determining trace elements in sponge silica (Ellwood et al. 2004, 2005) (Figs. 1, 4). Iron and aluminum were used as diagnostic elements for potential clay contamination of samples. Briefly, each slice was digested at 50°C in a hydrochloric acid–hydrogen peroxide (1 mol L<sup>-1</sup> : 10%) solution for 5 h to remove organic sponge mesohyl matrix. Slices were rinsed with deionized water and digested for 1 h in a hot (90°C) solution of hydroxylamine hydrochloride (0.1%) in acetic acid (1%); this was followed by digestion for a second hour in a solution of sodium fluoride (0.1%) in acetic acid (1%). The final cleaning step involved heating spicules in a strong acid solution (50%

$\text{HNO}_3$ :HCl, 1:1). Following cleaning, spicules were dissolved with hydrofluoric acid. Iron, zinc, and aluminum were determined in hydrofluoric digest by graphite furnace atomic adsorption spectrometry (Perkin Elmer 4100ZL), while silicon was determined colorimetrically.

$\Delta^{14}\text{C}$ —To determine the  $\Delta^{14}\text{C}$  signature of organic carbon trapped within sponge silica, approximately eight (~1-g) samples were removed from the lamella along the axis of growth adjacent to section B. To remove external organic mesohyl matrix, a slightly modified oxidative cleaning procedure, detailed in Singer and Shemesh (1995), was used. Briefly, samples were repeatedly digested at 65°C with a 1:1 nitric acid: perchloric acid mix for three 3-h periods. Between periods of digestion, samples were rinsed with Milli-Q water. At the end of the final period, the samples were left overnight at room temperature before the final Milli-Q water rinse. The  $\Delta^{14}\text{C}$  content of the silica in the samples was determined by accelerator mass spectrometry, under contract by the Rafter RadioCarbon Laboratory, Lower Hutt. Prior to analysis samples were dried, crushed, and then combusted at 900°C in sealed

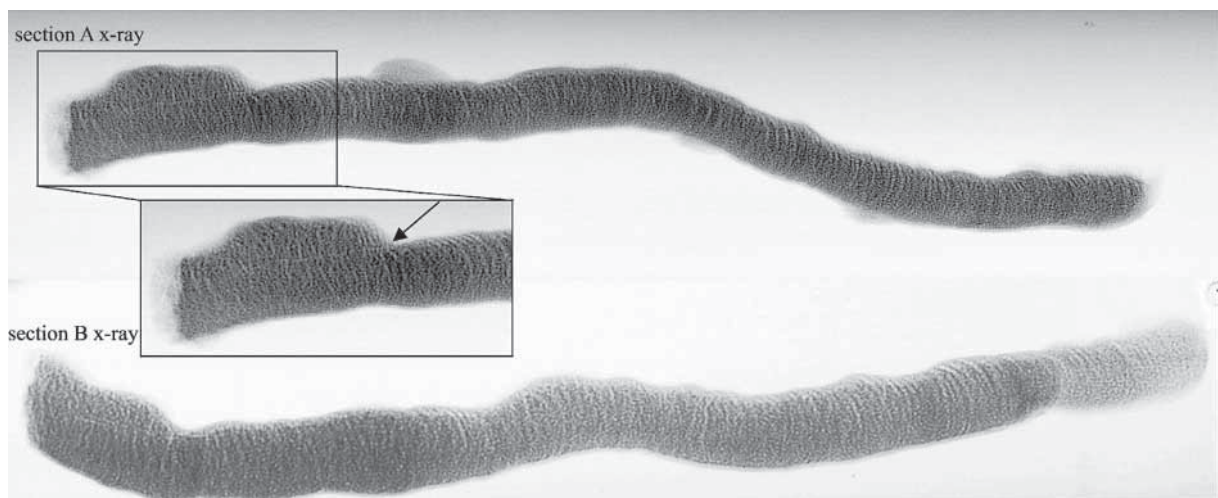


Fig. 4. X-rays of sections A and B removed from *Corallistes undulatus* Lévi and Lévi. Arrows in insert box indicate the boundary between the 'overgrowth' skeleton and the 'original' skeleton. Overgrowth material was removed prior to  $^{32}\text{Si}$  dating and Zn:Si determination. Note the alternating light and dark density band-pairs in both X-ray sections. Sections A and B were 175.9 mm and 147.4 mm long, respectively.

quartz tubes with cupric oxide and silver wire to liberate the carbon contained within the sponge desmas. The graphitization of the  $\text{CO}_2$  was carried out with hydrogen, with iron powder as the catalyst.

**Total organic carbon**—The amount of total organic mesohyl carbon associated with the sponge was estimated using a simple loss-on-ignition process. This involved removing three small pieces of siliceous skeletal material from the sponge, drying to a constant weight, and then combusting at  $450^\circ\text{C}$  overnight in a muffle furnace. After cooling samples were weighed again. To convert the amount of organic matter lost to an amount of organic carbon lost, we assumed that sponge organic matter is 40% carbon by weight.

## Results and discussion

**Enumeration of X-ray silica density bands**—X-ray analysis of sections A and B removed from opposite sides of the sponge lamella revealed a series of light and dark bands representing variation in the density of the silica in the desma skeleton, as manifested in the size, thickness, and orientation of the desma spicules. While the light and dark band-pairs in both sections appeared to be relatively regular, clear identification of bands in X-ray was not always easy with the unaided eye, as some bands were fuzzy. We estimate bands counts to vary by about  $\pm 10\%$ .

The lengths of sections A and B were 175.9 mm and 147.4 mm, respectively, yielding counts of 144 and 137 light and dark density band-pairs, respectively (Fig. 4). Thus, the average thickness of each band-pair was 1.2 mm/band-pair in Section A and 1.1 mm/band-pair in Section B, respectively.

**Band formation**—The concentric nature of these light and dark band-pairs raises questions regarding the mode of band formation and the time frame under which they are deposited. At the most basic level, spicule formation in sponges starts around an organic axial filament, which appears to act as a template to chemically and spatially direct nanoscale silica precipitation (Shimizu et al. 1998; Cha et al. 1999; Müller et al. 2003). This all occurs in membrane-enclosed vesicles.

On a larger scale, the 1.1–1.2-mm-wide band-pairs most likely represent several layers of desmas that vary in the thickness of their silica deposition (the dicranoclone desmas of *C. undulatus* are approximately  $600\ \mu\text{m}$  deep). The band-pairs would thus represent biannual seasonal variation in the deposition of silica, darker layers representing desmas that are less heavily siliceous than those in the lighter band-pair.

Based on the timescale for *C. undulatus* (see below), it would appear that desma layer formation occurs on a roughly biannual time frame, with layers being deposited at different densities, due perhaps to seasonal constraints in the availability of silica or food supply. Whether band formation occurs continuously or with defined stop periods (i.e., seasonally) within an annual time frame remains to be tested.

In plate-forming sponges there is every reason to believe that silica extension occurs in a linear fashion. Most sponges, whether massive or plate-shaped, grow outward

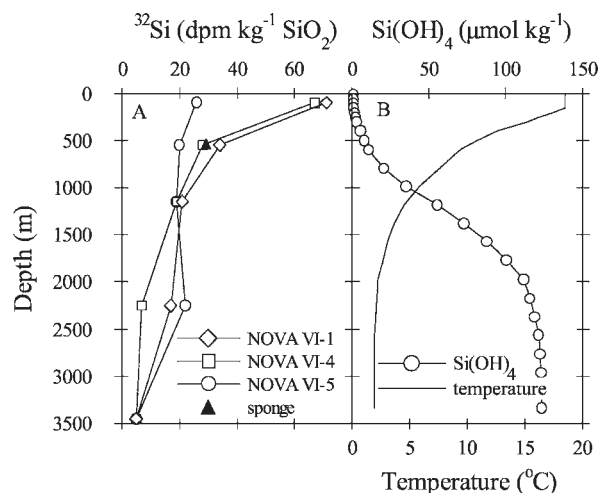


Fig. 5. (A)  $^{32}\text{Si}$  specific activity for the rim sample removed from *Corallistes undulatus* Lévi and Lévi and  $^{32}\text{Si}$  specific activities for water column profile stations sampled during the NOVA South Pacific Expedition (Somayajulu et al. 1973). (B) Profiles for  $\text{Si(OH)}_4$  concentration and water temperature versus depth for station 208-P06W.

from the surface, building upon the original surface and eventually incorporating it within the growing margin of the sponge. Where layers of desmas are added to the emerging margin, we have frequently observed differences in desma density in histological sections, some desmas being thin and fragile, others being fully siliceous.

Concentric layers are clearly visible in histological sections of the nonlithistid tropical species *Xestospongia testudinaria* Lamarck and of various species of *Petrosia* Vosmaer (Order Haplosclerida: Family Petrosiidae) as well. Very large cushion or barrel-shaped sponges often senesce in the central parts of the body as a result of the increasing inefficiency of the aquiferous system as the sponge grows larger (Kelly unpubl. data).

In lithistid sponges such as the tropical species *Theonella swinhoei* Gray and *Discodermia dissoluta* Schmidt (Family Theonellidae), the outer 3–5 mm of the external surface of the sponge is often quite soft, while the internal portions are stony. Histological sections reveal that the desmas are delicate, incomplete, and obviously actively accreting silica in this outer margin of the sponge.

**How are bands related to extension rate?**—To test whether bands were annular in nature,  $^{32}\text{Si}$  dating was attempted. The  $^{32}\text{Si}$  results showed some variability but are consistent with previous  $^{32}\text{Si}$  data from this region (Fig. 5) (Somayajulu et al. 1973). A general trend of decreasing  $^{32}\text{Si}$  activity with increasing length was found (Fig. 6; Table 1). To evaluate the extension rate of the sponge, we plotted  $^{32}\text{Si}$  activity versus length and then fitted the data to the following equation:

$$^{32}\text{Si} = ^{32}\text{Si}_0 \exp^{-\lambda Ax} \quad (1)$$

where  $^{32}\text{Si}$  and  $^{32}\text{Si}_0$  are measured and initial  $^{32}\text{Si}$  activities;

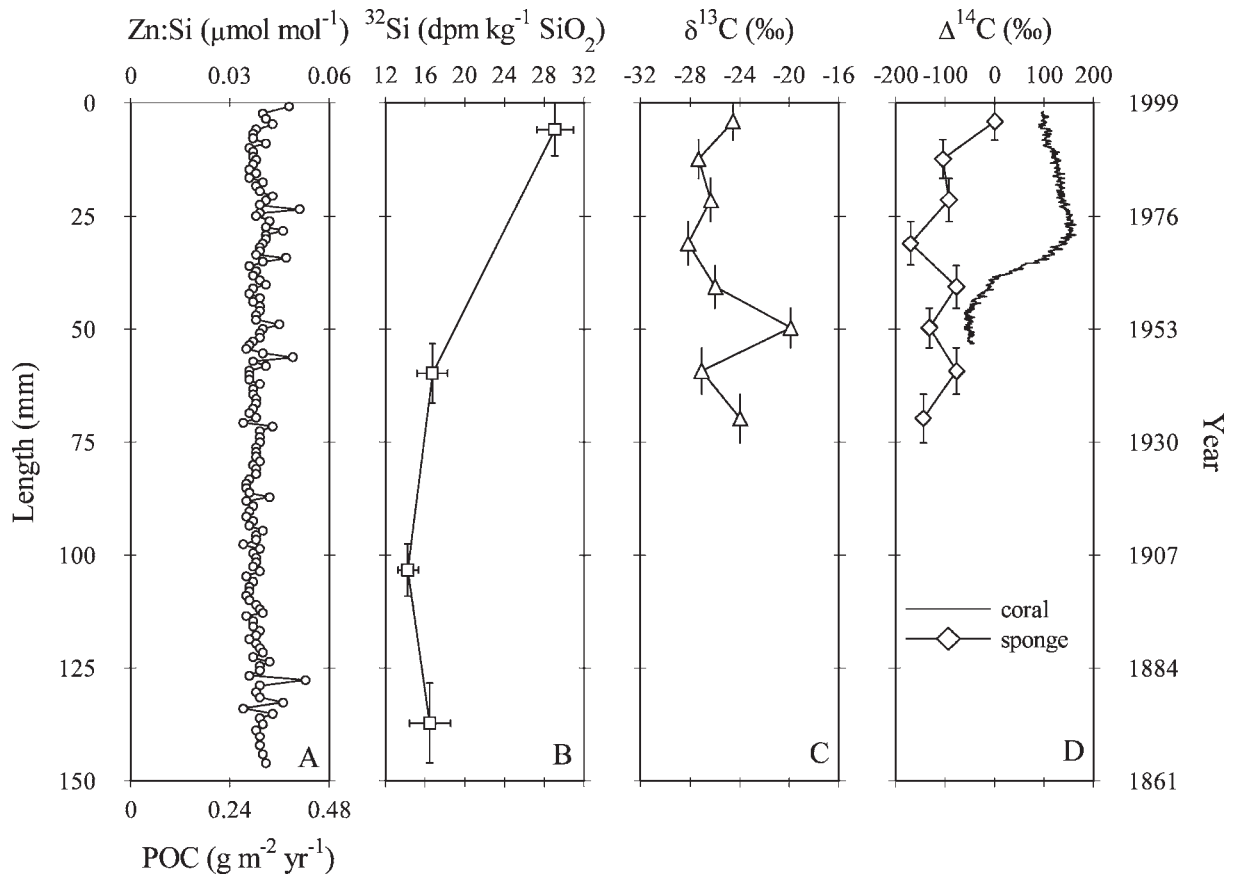


Fig. 6. (A) Zn:Si data versus length of sponge section B, from the outer margin. Note that there was no correlation between the zinc data and the data for iron and aluminum, thereby indicating that the cleaning procedure was effective in removing surface contaminants. The lower POC scale represents the estimated benthic POC flux reaching *Corallistes undulatus* Lévi and Lévi. (B)  $^{32}\text{Si}$  data for sections removed along the axis of growth. Error bars on the y-axis indicate the width of each segment removed, and on the x-axis, error bars represent  $1\sigma$  counting statistic errors. Note that the  $^{32}\text{Si}$  segment length data have been normalized to the Zn:Si length data. The normalization factor is 0.83. (C)  $\delta^{13}\text{C}$  data for carbon trapped within the silica matrix. Error bars on the y-axis indicate the width of each segment removed. (D)  $\Delta^{14}\text{C}$  data carbon trapped within the silica matrix versus length and age (right-hand axis). Error bars on the y-axis indicate the width of each segment removed. The age model developed for *C. undulatus* assumes a linear extension rate. This extension rate is based on a sponge age of 135 yr, with the length of section B measuring 147.4 mm. The high-resolution coral  $\Delta^{14}\text{C}$  record is for a large *Porites lutea* coral located in open marine conditions off Rarotonga, spanning the years from 1959 to 1997 (Guilderson et al. 2000). Note the increase in  $\Delta^{14}\text{C}$  from 1960 and 1970, resulting from the testing of nuclear weapons in the atmosphere.

$\lambda$  is the decay constant, set here with a half life of  $140 \pm 10$  yr (Morgenstern et al. 2001);  $x$  is the length (cm) along the analyzed section; and  $A$  is the reciprocal of the extension rate ( $\text{cm yr}^{-1}$ ). Using all the data, we obtained an extension rate of  $1.3 \text{ mm yr}^{-1}$  for section A and an extension rate of  $1.1 \text{ mm yr}^{-1}$  for section B, which gives an overall sponge age that ranges between  $\sim 135$  to 160 yr.

Such an age would indicate that the X-ray band-pairs (144 and 137) represent an annual deposition of silica. Although the  $^{32}\text{Si}$  data show some variability, especially with the last  $^{32}\text{Si}$  segment, which has a higher specific activity than its predecessor, the general trend of decreasing  $^{32}\text{Si}$  activity toward the base of the sponge is consistent with the silica deposition model described above.

Table 1. Silicon-32 ( $^{32}\text{Si}$ ) specific activity for silica ( $\text{SiO}_2$ ) segments removed from *Corallistes undulatus* Lévi and Lévi.

Silica segment (cm)*	Initial weight (g)	Purified $\text{SiO}_2$ (g)	Biogenic silica (%)	$^{32}\text{Si}$ specific activity ( $\text{dpm kg}^{-1} \text{SiO}_2$ )†
0–1.4	5.01	3.91	78.0	$29.08 \pm 1.84$
6.4–8.0	4.59	3.66	79.7	$16.70 \pm 1.52$
11.75–13.15	6.08	5.07	83.4	$14.27 \pm 1.01$
15.45–17.59	3.78	3.20	84.7	$16.47 \pm 2.09$

\* Distance from outer rim.

† Error represent  $1\sigma$  in counting statistics. dmp = disintegrations per minute.

Table 2.  $\Delta^{14}\text{C}$  and  $\delta^{13}\text{C}$  values for carbon trapped within silica ( $\text{SiO}_2$ ) segments removed from *Corallistes undulatus* Lévi and Lévi.

Sample ID No.	NZA*	Length (mm)†	Age	$\delta^{13}\text{C}$ (‰)	Radiocarbon age (yr)	$\Delta^{14}\text{C}$ (‰)
1	22881	0–8.12	1995.0 $\pm$ 3.6	–24.56	–60 $\pm$ 40 BP	0.8 $\pm$ 5.0
2	23291	8.12–16.68	1987.4 $\pm$ 4.0	–27.34	829 $\pm$ 40 BP	–104.1 $\pm$ 4.7
3	23292	16.68–26.28	1978.9 $\pm$ 4.5	–26.34	721 $\pm$ 40 BP	–91.9 $\pm$ 4.3
4	23293	26.28–35.91	1969.7 $\pm$ 4.7	–28.16	1442 $\pm$ 65 BP	–169.9 $\pm$ 6.9
5	23294	35.91–45.34	1960.6 $\pm$ 4.4	–25.97	593 $\pm$ 40 BP	–77.4 $\pm$ 4.4
6	23295	45.34–54.17	1951.9 $\pm$ 4.3	–19.90	1078 $\pm$ 45 BP	–131.4 $\pm$ 4.9
7	23296	54.17–64.44	1942.7 $\pm$ 4.9	–27.07	586 $\pm$ 45 BP	–76.5 $\pm$ 5.0
8	23009	64.44–75.12	1932.6 $\pm$ 5.3	–23.96	1200 $\pm$ 150 BP	–144.1 $\pm$ 15.5

\* Laboratory code.

† Distance from outer rim. BP = before present (years before 1950).

Using the maximum extension rate of 1.3 mm yr<sup>–1</sup>, a sponge diameter of 30 cm, a height of 20 cm, and a wall thickness of 15 mm, the amount of silica ( $\text{SiO}_2$ ) required for growth is about 15 g per year. This raises the following question: Is *C. undulatus* capable of pumping enough water to acquire 15 g of  $\text{SiO}_2$  from seawater for desma formation?

The typical pumping rate for marine sponges varies between 1 and 11 mL min<sup>–1</sup> cm<sup>–3</sup> (Yahel et al. [2003] and references therein). Using these values as extremes and a calculated total volume of 1,005 cm<sup>3</sup> for *C. undulatus*, we calculate a pump rate ranging between 1 and 11 L min<sup>–1</sup>. The estimated dissolved silicon concentration at the sponge site is 8  $\mu\text{mol L}^{-1}$  (Fig. 5). Assuming that *C. undulatus* deposits 15 g of  $\text{SiO}_2$  per year, a minimum of 125,000 liters of water must be filtered per year, assuming that *C. undulatus* effectively removes 25% of the silicon from the water that it pumps. Converting this volume (125,000 liters) to a pump rate produces a value of 0.2 L min<sup>–1</sup>, which is well below the range of 1 to 11 L min<sup>–1</sup>. Based on this calculation, it appears that *C. undulatus* is more than capable of filtering enough water to acquire the silicon required for skeleton formation. Indeed, this value of 0.2 L min<sup>–1</sup> should be regarded as a minimum pump rate, as it is well below the range of 1 to 11 L min<sup>–1</sup> based on other sponges species (Yahel et al. [2003] and references therein).

In order to check this, we also calculated the uptake of silicon based on published silicon uptake rates for the marine sponge *Halichondria panicea* in Reincke and Barthel (1997). While *C. undulatus* is considerably different phylogenetically than *H. panicea*, it is still useful to estimate the time required to acquire the 15 g of  $\text{SiO}_2$  from seawater with a silicon concentration equal to 8  $\mu\text{mol L}^{-1}$ . Using a Michaelis–Menten approach and the values of 19.33  $\mu\text{mol h}^{-1}$  (per gram of dried sponge) and 46.4  $\mu\text{mol L}^{-1}$  for the maximum uptake rate and the half-saturation constant, respectively (Reincke and Barthel 1997), an uptake rate of 2.84  $\mu\text{mol h}^{-1}$  (per gram of dried sponge) is calculated for *C. undulatus*. Using an annual deposited dry weight of 18.5 g (15 g of  $\text{SiO}_2$  plus 3.5 g of organic material), the rate of silicon uptake is estimated at 52.6  $\mu\text{mol h}^{-1}$  or 27.6 g ( $\text{SiO}_2$ ) yr<sup>–1</sup>. In other words, it takes *C. undulatus* 197 d to acquire 15 g of  $\text{SiO}_2$ . Again, this basic calculation indicates that *C. undulatus* is capable of acquiring enough silicon from surrounding seawater to support an extension rate of 1.3 mm yr<sup>–1</sup>.

*Validity of the <sup>32</sup>Si dating technique*—There has been some debate about the validity of the previously published <sup>32</sup>Si water column data (Fig. 5) (Peng et al. 1993; Craig et al. 2000). The <sup>32</sup>Si data for *C. undulatus* agrees well with the water column data from Somayajulu et al. (1973). Such an agreement can only strengthen the case for the NOVA and the GEOSECS <sup>32</sup>Si data sets (Somayajulu et al. 1973, 1987, 1991). The close agreement between the water column data and the sponge data generated in this study indicates that there is certainly nothing wrong with the <sup>32</sup>Si technique, merely with how the data should be interpreted (Craig et al. 2000).

*Basic carbon requirement*—Taking the <sup>32</sup>Si data set at face value indicates that the silica density banding seen by X-ray analysis reflects an annual, and seasonally variable, deposition of silica in the desma skeleton, resulting in pairs of light and dark bands, somewhat similar to the seasonal deposition of aragonite in corals. However, unlike corals that live in surface waters, where variables such as temperature, sunlight exposure, and nutrient concentrations vary seasonally, variations in such physical and chemical parameters are likely to be more subtle at a depth of 540 m.

The organic carbon requirement for *C. undulatus* is based on the total organic content of the sponge, which is 19.2%  $\pm$  0.3%. Assuming an extension rate of 1.3 mm yr<sup>–1</sup> (which corresponds to about 15 g of  $\text{SiO}_2$  deposited each year in the latter years of growth), the amount of carbon required to support this is about 1.2 g yr<sup>–1</sup>. (Note that this assumption does not include organic carbon required for cell maintenance, mesohyl regeneration, or respiration, which is by far the largest carbon expenditure within the sponge. Thus, this value should be regarded as a lower estimate.)

*Food sources to C. undulates*—To determine the links between food and growth rate we explored the likely food sources to *C. undulatus* using the  $\Delta^{14}\text{C}$  and  $\delta^{13}\text{C}$  signature of organic material trapped within the desma matrix and the Zn:Si ratio of the silica (see below). If the maximum extension rate of 1.3 mm yr<sup>–1</sup> measured for *C. undulatus* is linked to food supply (e.g., the flux of phytodetritus [labile dissolved and particulate carbon]) from overhead waters and organic carbon acquired from its surrounds, it is important to understand the exact proportions each source

Table 3. Range of  $\Delta^{14}\text{C}$  and  $\delta^{13}\text{C}$  values for the organic carbon pools of various constituents, except for the water values, which are for the inorganic carbon pool.

Constituent	$\Delta^{14}\text{C}$ (‰)*	$\delta^{13}\text{C}$ (‰)*
Sponge	-169.9 to 0.8	-17 to -25
Water		
Surface	~100	~0
Deep, 540 m	~20	~0
Zooplankton/phytoplankton	~60–80	-18 to -26
POC full water column†	52 to -86	-20 to -25
DOC water column below 200 m	-450 to -550	~-22
Sediment		
Flocculent layer (2–4 mm)	~-245	~-22
0.2–10 cm	~-240 to -600	~-22

\*  $\Delta^{14}\text{C}$  and  $\delta^{13}\text{C}$  values are taken from Bauer et al. (1998), Druffel et al. (1998), Druffel and Williams (1990), Druffel et al. (1992), Key et al. (1996), and Wang et al. (1998).

† POC, particulate organic carbon; DOC, dissolved organic carbon.

contributes to the overall amount of organic carbon taken up by the sponge (Billet et al. 1983; Reiswig 1985; Yahel et al. 2003).

*Surface ocean supply of organic carbon*—The  $\Delta^{14}\text{C}$  of carbon trapped in sponge silica had values that range between  $-169.9\text{‰} \pm 6.9\text{‰}$  and  $0.8\text{‰} \pm 5\text{‰}$  (Fig. 6; Table 2). For the four samples covering the period from 1970 to the present day,  $\Delta^{14}\text{C}$  values were well below the current  $\Delta^{14}\text{C}$  signature of surface waters for the oceanic region (Fig. 6; Table 3). If the main organic carbon source being captured by this sponge was predominantly of a surface ocean source, then one would expect it to have a positive signature for the organic carbon trapped with desmas deposited after the 1960s where the surface ocean signal was, and still is, strongly influenced by  $^{14}\text{C}$  produced during the atmospheric testing of nuclear weapons in the 1950s and 1960s (Fig. 6; Table 3) (Guilderson et al. 2000; Broecker 2004).

These low  $\Delta^{14}\text{C}$  values in *C. undulatus* subsequent to the era of atmospheric nuclear weapons testing raises the following question: Where does this sponge acquire its carbon for growth? Close inspection of the  $\Delta^{14}\text{C}$  and  $\delta^{13}\text{C}$  results indicates that the dominant carbon source is not directly derived from the inorganic carbon pool (Table 3).

The  $\delta^{13}\text{C}$  signal is well negative of the 0‰ expected for the carbonate, bicarbonate pool, although the  $\Delta^{14}\text{C}$  values for the last section of the sponge are similar to water column values (Table 3) (Key et al. 1996). Rather, the  $\delta^{13}\text{C}$  values obtained for *C. undulatus* are consistent with the consumption of organic material of a biological origin (Druffel et al. 1998; Wang et al. 1998).

It is, however, unlikely that fresh surface-derived zooplankton and phytoplankton material was the major source of organic carbon to *C. undulatus*. Present-day  $\Delta^{14}\text{C}$  values measured for zooplankton and phytoplankton are usually around 60–80‰, while the  $\Delta^{14}\text{C}$  for *C. undulatus* is much less (Fig. 6; Table 3) (Druffel et al. 1992, 1998; Wang et al. 1998).

Other potential organic carbon sources to *C. undulatus* include aged organic material such as detrital aggregates and sediment-derived organic seston, and refractory dissolved organic carbon (DOC), which can have quite variable  $\Delta^{14}\text{C}$  signatures (Wang et al. 1998; Wang and Druffel 2001). The total organic  $\Delta^{14}\text{C}$  signatures for these constituents cover a large range from about -240‰ to -600‰ (Table 3) (Wang et al. 1996, 1998; Wang and Druffel 2001). Although these bulk organic carbon values are more negative compared with the  $\Delta^{14}\text{C}$  seen for *C. undulatus*, they are unlikely to reflect the 'true'  $\Delta^{14}\text{C}$  signature of the organic carbon being consumed by this sponge. The  $\Delta^{14}\text{C}$  signature of specific groups of compounds within sediment flocculent and surficial sediment layers varies considerably; more labile material with a high nutritional value tends to have a more positive  $\Delta^{14}\text{C}$  signature than the total organic carbon signature. For instance, the  $\Delta^{14}\text{C}$  values for carbohydrates, proteins/amino acids, and lipids range from -94‰ to -186‰, from -52‰ to -140‰, and from -170‰ to -417‰, respectively (Wang et al. 1998).

The most plausible explanation for the  $\Delta^{14}\text{C}$  values seen for *C. undulatus* is that they result from the sponge consuming a mixed diet of fresh surface-derived material with a more positive  $\Delta^{14}\text{C}$  signature and older, perhaps sediment-derived material with a more negative  $\Delta^{14}\text{C}$  signature. Based on the  $\Delta^{14}\text{C}$  values seen for samples postdating the 1970s, the direct contribution of surface-derived material to the *C. undulatus* diet is minor. If this material was a major component, an immediate shift in  $\Delta^{14}\text{C}$  from more negative values to more positive values would be expected from about 1970 onward; such an increase in  $\Delta^{14}\text{C}$  signal is only seen in the sample taken from the outer rim of the foliose bowl (Fig. 6). The lack of increase in  $\Delta^{14}\text{C}$  for second and third samples removed from the outer rim of the bowl indicates that the time frame for fresh, labile organic material rich in 'bomb'  $^{14}\text{C}$  to be incorporated into the general organic carbon pool is on the order of decades, at least in oligotrophic areas, where productivity and particulate organic carbon (POC) export is low.

While  $\Delta^{14}\text{C}$  data indicates that the amount of "fresh" surface-derived organic material incorporated into *C. undulatus* is low, it is important to try and gauge exactly how much surface export is likely to contribute to the overall carbon budget. Recent work has shown that the zinc content of sponge silica can be used to estimate POC export (Ellwood et al. 2004, 2005). While sponges are not passive POC collectors (i.e., they can actively pump hundreds to thousands of liters of water per day, depending on pump rate and sponge size), the zinc content of their spicules is related to POC export (Ellwood et al. 2004, 2005). This relationship can be described using a distribution factor of  $8.1 \text{ g m}^{-2} \text{ yr}^{-1} \mu\text{mol}^{-1} \text{ mol}$ , which was obtained by correlating the zinc content of sponges to nearby sediment-trap POC flux estimates (Ellwood et al. 2005).

Using an average Zn:Si value of  $0.039 \pm 0.003 \mu\text{mol mol}^{-1}$  for *C. undulatus* silica, and then multiplying by  $8.1 \text{ g m}^{-2} \text{ yr}^{-1} \mu\text{mol}^{-1} \text{ mol}$ , and allowing for POC degradation with depth, we estimate a surface export POC flux of

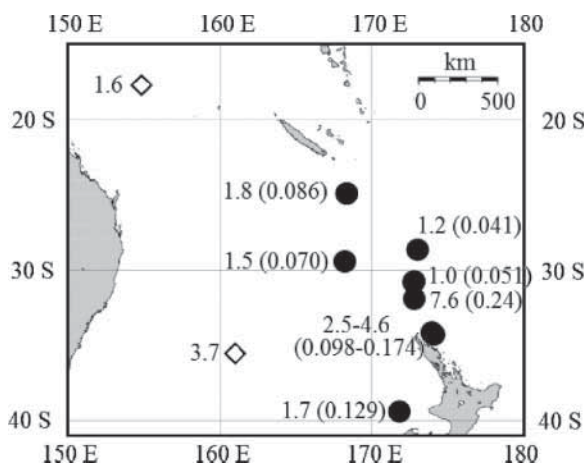


Fig. 7. Map showing Zn:Si ( $\mu\text{mol mol}^{-1}$ ) (numbers in brackets) and estimated surface POC export flux ( $\text{g m}^{-2} \text{yr}^{-1}$ ) for the lithistid sponge species *Neoschrammeniella fulvodesmus* (Lévi and Lévi) and *Reidispongia coerulea* Lévi and Lévi, collected from around and north of New Zealand. Also shown is the estimated surface POC export flux for sediment trap sites 12 and 13 (diamonds) (Kawahata and Ohta 2000). Surface POC export fluxes for lithistid sponges were estimated using the following relationship:  $\text{POC} = \text{Zn} : \text{Si} (\mu\text{mol mol}^{-1}) \times 8.1 (\text{g m}^{-2} \text{yr}^{-1} \text{mol}^{-1} \mu\text{mol}^{-1})$ , and correcting for degradation with depth using the Martin POC versus depth relationship (Ellwood et al. 2005).

around  $0.8 \text{ g m}^{-2} \text{yr}^{-1}$ . This calculated export flux is low and consistent with the oligotrophic nature of this oceanic region; it is also consistent with other POC export estimates based on the zinc content of other lithistid sponges and with sediment-trap results for the Tasman Sea, Coral Sea region (Fig. 7) (Kawahata and Ohta 2000).

Using the surface export values derived from proxy and sediment-trap results (Figs. 6, 7), correcting for depth using the Martin export equation (Martin et al. 1987) and assuming a sponge collection area of  $0.071 \text{ m}^2$ , based on a 15-cm diameter, the amount of organic carbon reaching *C. undulatus* per annum is between about 0.018 and 0.100 g. This estimate is well below the minimum annual organic carbon requirement of *C. undulatus*. Using the maximum of 0.100 g, the amount of surface-derived material only constitutes 8% of the 1.2 g required for growth. This result complements the  $\Delta^{14}\text{C}$  results, which do not show a strong surface ocean signal (Fig. 6). The remaining 92% of the organic material required by the sponge is likely to come from older, perhaps sediment-derived material, which has a modified  $\Delta^{14}\text{C}$  signature.

The low surface export POC signal raises the question as to what triggers light and dark band-pair formation. Because our sample resolution of *C. undulatus* was roughly annual, we are unable to identify whether seasonal export events are the trigger for desma formation. Longer term, no correlation was observed between the Zn:Si data and climate indices such as the El Niño–Southern Oscillation, thereby indicating that this phenomenon does not play a major role in triggering desma formation.

It should be noted that the benthic fauna at the seamount from which this sponge was collected was particularly rich, even though overhead waters are oligo-

trophic. Similar anomalous results in the abundance of deep-sea fauna have been found at other sites exposed to strong current regimes (Genin et al. 1992). Enhancement of faunal numbers appears to result from an increased flux of food material to and through the feeding organs of the animal, and the removal of sediment seems to be associated with increased current speed. Furthermore, lithistid sponges prefer hard substrates for colonization and low sedimentation environments to reduce the chance of burial under nonorganic material. The site at which *C. undulatus* was collected certainly warrants further study to understand the links between benthic food supply and the health and vitality of the benthic community.

X-ray analysis of two siliceous sections removed from the tropical deep-ocean sponge *C. undulatus* showed approximately 140 light and dark density band-pairs within the skeleton structure. The age of the sponge, as estimated using  $^{32}\text{Si}$  dating technique, indicates that *C. undulatus* is aged between ca. 135 and 160 yr, thereby indicating that silica banding represents an annual deposition of silica in the desma skeleton.

Using the  $\Delta^{14}\text{C}$  signature of organic material trapped within the spicule matrix and the zinc content of the spicule matrix to explore the links between food supply and sponge growth, we found that the supply of POC from the surface ocean is insufficient to support sponge growth. A carbon budget developed using these results indicates that the main source of organic carbon to *C. undulatus* appears to come from mixed sources, with fresh, labile surface ocean material being the minor source and older, perhaps more-refractory material being the dominant source.

## References

- AIZENBERG, J., J. C. WEAVER, M. S. THANAWALA, V. C. SUNDAR, D. E. MORSE, AND P. FRATZL. 2005. Skeleton of *Euplectella* sp.: Structural hierarchy from the nanoscale to the macroscale. *Science* **309**: 275–278.
- BAUER, J. E., E. R. M. DRUFFEL, P. M. WILLIAMS, D. M. WOLGAST, AND S. GRIFFIN. 1998. Temporal variability in dissolved organic carbon and radiocarbon in the eastern North Pacific Ocean. *J. Geophys. Res. Oceans* **103**: 2867–2881.
- BILLET, D. S. M., R. S. LAMPITT, A. L. RICE, AND R. F. C. MANTOURA. 1983. Seasonal sedimentation of phytoplankton to the deep-sea benthos. *Nature* **302**: 520–522.
- BROECKER, W. S. 2004. 4.09 Radiocarbon, p. 245–260. In H. D. Holland and K. K. Turekian [eds.], *Treatise on geochemistry* Elsevier Pergamon.
- CHA, J. N., AND OTHERS. 1999. Silicatein filaments and subunits from a marine sponge direct the polymerization of silica and silicones in vitro. *Proc. Natl. Acad. Sci. USA* **96**: 361–365.
- CRAIG, H., B. L. K. SOMAYAJULU, AND K. K. TUREKIAN. 2000. Paradox lost: Silicon 32 and the global ocean silica cycle. *Earth Planet. Sci. Lett.* **175**: 297–308.
- DRUFFEL, E. R. M., S. GRIFFIN, J. E. BAUER, D. M. WOLGAST, AND X.-C. WANG. 1998. Distribution of particulate organic carbon and radiocarbon in the water column from the upper slope to the abyssal NE Pacific Ocean. *Deep-Sea Res. II* **45**: 667–687.
- , AND P. M. WILLIAMS. 1990. Identification of a deep marine source of particulate organic carbon using bomb  $^{14}\text{C}$ . *Nature* **347**: 172–174.

- , P. M. WILLIAMS, J. E. BAUER, AND H. ERTEL. 1992. Cycling of dissolved and particulate organic matter in the open ocean. *J. Geophys. Res. Oceans* **97**: 15639–15659.
- ELLWOOD, M. J., M. KELLEY, H. NEIL, AND S. D. NODDER. 2005. Reconstruction of paleo-particulate organic carbon fluxes for the Campbell Plateau region of southern New Zealand using the zinc content of sponge spicules. *Paleoceanography* **20**: PA3010, doi:10.1029/2004PA001095.
- , M. KELLEY, S. D. NODDER, AND L. CARTER. 2004. Zinc/silicon ratios of sponges: A proxy for carbon export to the seafloor. *Geophys. Res. Lett.* **31**: L12308, doi:10.1029/2004GL019648.
- GENIN, A., C. K. PAULL, AND W. P. DILLON. 1992. Anomalous abundances of deep-sea fauna on a rocky bottom exposed to strong currents. *Deep-Sea Res.* **39**: 293–303.
- GOODAY, A. J., AND C. M. TURLEY. 1990. Responses by benthic organisms to inputs of organic material to the ocean floor: A review. *Philos. Trans. R. Soc. Lond. A* **331**: 119–138.
- GUILDERSON, T. P., D. P. SCHRAG, E. GODDARD, M. KASHGARIAN, G. M. WELLINGTON, AND B. K. LINSLEY. 2000. Southwest subtropical Pacific surface water radiocarbon in a high-resolution coral record. *Radiocarbon* **42**: 249–256.
- KAWAHATA, H., AND H. OHTA. 2000. Sinking and suspended particles in the south-west Pacific. *Mar. Freshw. Res.* **51**: 113–126.
- KELLY, M. 2000. Description of a new lithistid sponge from northeastern New Zealand, and consideration of the phylogenetic affinities of families Corallistidae and Neopeltidae. *Zoosystema* **22**: 265–283.
- . 2003. Revision of the sponge genus *Pleroma Sollas* (Lithistida: Megamorina: Pleromidae) from New Zealand and New Caledonia, and description of a new species. *N. Z. J. Mar. Freshw. Res.* **37**: 113–127.
- . In press. The marine fauna of New Zealand: Porifera: 'Lithistid' Demospongiae. NIWA Biodiversity Memoir 121.
- KEY, R. M., P. D. QUAY, G. A. JONES, A. P. McNICHOL, K. F. VONREDE, AND R. J. SCHNEIDER. 1996. WOCE AMS radiocarbon. 1. Pacific Ocean results (P6, P16 and P17). *Radiocarbon* **38**: 425–518.
- LAL, D., E. D. GOLDBERG, AND M. KOIDE. 1960. Cosmic-ray-produced silicon-32 in nature. *Science* **131**: 332–337.
- , V. N. NIJAMPURKAR, AND B. L. K. SOMAYAJULU. 1970. Concentration of cosmogenic  $^{32}\text{Si}$  in deep Pacific and Indian waters based on study of *Galathea* deep-sea siliceous sponges. *Galathea Rep.* **11**: 247–256.
- LÉVI, C., J. L. BARTON, E. LEBRAS, AND P. LEHUEDE. 1989. A remarkably strong natural glass rod: The anchoring spicule of the *Monorhaphis* sponge. *J. Mater. Sci. Lett.* **8**: 337–339.
- , AND P. LÉVI. 1983. Eponges Tetractinellides et Lithistides bathyales de Nouvelle Calédonie. *Bull. Mus. Natl. Hist. Nat. Paris* **4**: 101–168.
- MARTIN, J. H., G. A. KNAUER, D. M. KARL, AND W. W. BROENKOW. 1987. VERTEX—carbon cycling in the Northeast Pacific. *Deep-Sea Res. Oceanogr. A* **34**: 267–285.
- MORGENSTERN, U., M. A. GEYH, H. R. KUDRASS, R. G. DITCHEBURN, AND I. J. GRAHAM. 2001. Si-32 dating of marine sediments from Bangladesh. *Radiocarbon* **43**: 909–916.
- MÜLLER, W. E. G., A. KRASKO, G. LE PENNEC, AND H. C. SCHRODER. 2003. Biochemistry and cell biology of silica formation in sponges. *Microsc. Res. Tech.* **62**: 368–377.
- PENG, T. H., E. MAIER-REIMER, AND W. S. BROECKER. 1993. Distribution of  $^{32}\text{Si}$  in the world ocean: Model compared to observation. *Global Biogeochem. Cycles* **7**: 463–474.
- POMPONI, S. A., M. KELLY, J. K. REED, AND A. WRIGHT. 2001. Diversity and bathymetric distribution of lithistid sponges in the tropical western Atlantic region. *Bull. Biol. Soc. Wash.* **10**: 344–353.
- REINCKE, T., AND D. BARTHEL. 1997. Silica uptake kinetics of *Halichondria panicea* in Kiel Bight. *Mar. Biol.* **129**: 591–593.
- REISWIG, H. M. 1985. In situ feeding in two shallow-water hexactinellid sponges, p. 504–510. *In* K. Rutzler [ed.], *New perspectives in sponge biology. Proceedings of the Third International Conference on the Biology of Sponges* (Woods Hole) Smithsonian Institute.
- SHIMIZU, K., J. CHA, G. D. STUCKY, AND D. E. MORSE. 1998. Silicatein alpha: Cathepsin L-like protein in sponge biosilica. *Proc. Natl. Acad. Sci. USA* **95**: 6234–6238.
- SINGER, A. J., AND A. SHEMESH. 1995. Climatically linked carbon-isotope variation during the past 430,000 years in Southern-Ocean sediments. *Paleoceanography* **10**: 171–177.
- SOMAYAJULU, B. L. K., D. LAL, AND H. CRAIG. 1973. Silicon-32 profiles in the South Pacific. *Earth Planet. Sci. Lett.* **18**: 181–188.
- , R. RENGARAJAN, D. LAL, AND H. CRAIG. 1991. GEOSECS Pacific and Indian Ocean  $^{32}\text{Si}$  profiles. *Earth Planet. Sci. Lett.* **107**: 197–216.
- , ———, ———, R. F. WEISS, AND H. CRAIG. 1987. GEOSECS Atlantic  $^{32}\text{Si}$  profiles. *Earth Planet. Sci. Lett.* **85**: 329–342.
- SUNDAR, V. C., A. D. YABLON, J. L. GRAZUL, M. ILAN, AND J. AIZENBERG. 2003. Fibre-optical features of a glass sponge. *Nature* **424**: 899–900.
- TYLER, P. A. 1995. Conditions for the existence of life at the deep-sea floor: An update. *Oceanogr. Mar. Biol. Annu. Rev.* **33**: 221–244.
- WANG, X.-C., AND E. R. M. DRUFFEL. 2001. Radiocarbon and stable carbon isotope compositions of organic compound classes in sediments from the NE Pacific and Southern Oceans. *Mar. Chem.* **73**: 65–81.
- , ———, AND C. LEE. 1996. Radiocarbon in organic compound classes in particulate organic matter and sediment in the deep northeast Pacific Ocean. *Geophys. Res. Lett.* **23**: 3583–3586.
- , ———, S. GRIFFIN, C. LEE, AND M. KASHGARIAN. 1998. Radiocarbon studies of organic compound classes in plankton and sediment of the northeastern Pacific Ocean. *Geochim. Cosmochim. Acta* **62**: 1365–1378.
- YAHIEL, G., J. H. SHARP, D. MARIE, C. HASE, AND A. GENIN. 2003. In situ feeding and element removal in the symbiont-bearing sponge *Theonella swinhoei*: Bulk DOC is the major source for carbon. *Limnol. Oceanogr.* **48**: 141–149.

Received: 31 October 2006

Accepted: 14 May 2007

Amended: 5 June 2007